

Tensile testing of primary plant cells and tissues

Amir J Bidhendi¹, Anja Geitmann^{1,2,*}

¹Institut de recherche en biologie végétale, Département de sciences biologiques
Université de Montréal, Montreal, Quebec, H1X 2B2, Canada

²Department of Plant Science, McGill University, Macdonald Campus, 21111 Lakeshore, Ste-Anne-de-Bellevue, Québec H9X 3V9, Canada

*Address correspondence to: Anja Geitmann (geitmann.aes@mcgill.ca)

Cite as: Bidhendi AJ, Geitmann A. 2018. Tensile testing of primary plant cells and tissues. In: Plant Biomechanics - From Structure to Function at Multiple Scales. Geitmann A, Gril J (eds), Springer Verlag, pp 321-347

Abstract

The primary cell wall controls plant growth and morphogenesis but also determines the structural resilience of non-woody plant organs. The predominant mechanical role of the primary cell wall lies in its ability to resist or conform to tensile forces. Assessing the tensile properties of the cell wall, therefore, is a fundamental feature from both biomechanics and mechanobiology perspectives. Tensile testing is a classic approach for the mechanical characterization of materials. Various loading strategies such as monotonic or cyclic loading or creep or relaxation allow for analysis of the material response in terms of elastic, viscoelastic and failure properties. Here, we discuss tensile testing strategies for plant samples with primary cell walls with the aim to provide a practical guide that highlights challenges and offers solutions for the design, execution and interpretation of such tests.

Keywords: Mechanical characterization, micromechanics, cell wall mechanics, tension test, uniaxial tensile test, biaxial testing, Young's modulus, cellulose, primary cell wall, anisotropy, inverse finite element analysis, multiscale, *Arabidopsis*

Introduction

Mechanical testing of material is an essential element in the toolbox of biomechanical research. Understanding how wood breaks, how it resists compression and bending stresses is essential in its use as a construction material or to understand how trees respond to external stresses such as wind and gravity. The resistance to damage of fruit after harvest determines the storage and handling procedures. To be meaningful, mechanical tests should mimic relevant stress types that the biological material experiences during its lifetime. Typical tests for woody plant tissues are three-point bending or compression tests, whereas fruits are typically tested under compression or impact loading.

The mechanical properties of plant tissues are not only relevant for the plant to withstand and respond to externally applied forces but are also involved in internal processes such as plant development and differentiation. The primary cell wall, characteristic of growing cells, is typically between a few tens of nanometers up to a few microns depending on the species, the organ of interest

as well as cell type (Derbyshire et al., 2007; Zamil et al., 2013). During plant development, at a cellular scale, the forces driving cellular expansion are generated internally by the turgor pressure that acts on the inner face of primary cell walls. As a result of this, a net permanent expansion of the cell wall results under tension that is interpreted as growth. To be consistent with this stress type, the methods used to measure the mechanical properties of plant material in the context of developmental processes need to relate to the tensile behavior of the cell wall. Such pertinent mechanical tests not only provide information on the mechanical behavior of the plant materials regarding stiffness or failure but also produce vital ingredients for mathematical models. Modeling approaches such as those based on finite element (FE) method attempt to explore phenomena such as cell growth, morphogenesis or organogenesis to elucidate the underlying biology or to guide future experimental strategies (Bidhendi and Geitmann, 2018). The quality of the predictions made by models are greatly augmented if actual quantitative information can be obtained from mechanical tests. In this chapter, the focus is on tensile testing related to primary plant tissues. The concepts of tensile testing, an introductory guide to tensile experiment components, and the challenges involved in its implementation are discussed.

Woody plant tissues are formed by the secondary xylem, a tissue that, depending on the species, comprises only a few different cell types most of which have lignified cell walls. From a macroscopic point of view, wood tissues are therefore relatively homogenous. Depending on the scale at which measurements are performed, a block of wood behaves relatively uniformly albeit with significant anisotropy because of the longitudinal arrangements of cells and the presence of growth rings. Interpretation of tensile test results of entire tissues can, therefore, be used to deduce the mechanical properties of single cells in relatively straightforward manner. Herbaceous plant organs, on the other hand, possess different types of tissues including turgid primary tissues such as parenchyma, collenchyma and sclerenchymatous tissues such as primary xylem. Because of this heterogeneous composition, the analysis of tensile tests administered to whole primary organs needs to consider the spatial variation of mechanical behavior within the organ. Similar considerations are made in Chapter 3 for bending tests.

The mechanics of woody tissue is dominated by the lignin and cellulose-rich secondary wall of the sclerenchymatous wood cells. Primary plant cell walls, on the other hand, are composed of several types of polysaccharides, proteins, ions and a significant amount of water. Lignin is absent from the primary wall, and cellulose, while abundant, is less organized and dominant than in the secondary wall. Cellulose is still considered to be a major load-bearing component, however, since due to a low tensile compliance its spatial arrangement can determine the magnitude and orientation of anisotropy in the cell wall (Baskin, 2005; Cosgrove, 2005). Because of the biochemical complexity of the material, the roles of polymers other than cellulose are rather prominent in defining the mechanics of primary plant cell wall (Bidhendi and Geitmann, 2016). The chemical configuration of pectin, for instance, is associated with the regulation of cell and tissue growth (Bidhendi and Geitmann, 2016; Palin and Geitmann, 2012), organogenesis and the ripening of fruits (Prasanna *et al.*, 2007). The visualization of cell wall polysaccharides has therefore been an important tool to understand plant cell structural makeup. However, in many studies, the spatial information on the distribution of cell wall components has been used directly to make inferences on cell mechanics which, unless accompanied by mechanical testing data, remain inconclusive. The reason is that the relationship between the chemical changes and mechanics is not straightforward. Highly methylesterified pectin in the tip where the growth occurs in pollen tubes is associated with a low stiffness as shown by

microindentation techniques (Chebli *et al.*, 2012; Zerzour *et al.*, 2009). Yet, pectin de-esterification is found to be associated with local softening in the shoot apical meristem where it seems to be a prerequisite for organogenesis or growth anisotropy (Braybrook and Peaucelle, 2013; Peaucelle *et al.*, 2015). This is not to mention the ultrastructural changes in the cell, such as changes in wall thickness or cell shape that are often not accounted for in studies focusing on the chemistry of wall polymer alone (Bidhendi and Geitmann, 2018). Therefore, visualization of cell wall composition needs to be associated with mechanical tests and *in silico* experiments to determine the consequence of specific changes in cell wall chemistry (Bidhendi and Geitmann, 2016).

The mechanics of the primary plant cell wall regulate both irreversible and reversible plant processes. Among the reversible processes are those regulating the opening and closing of stomatal guard cells or the pulvini-driven motion of plant leaves. While *in silico* modeling has helped to understand the mechanical underpinnings of these mechanisms (Bidhendi and Geitmann, 2018; Cooke *et al.*, 1976; Forterre *et al.*, 2005), limited experimental work exists to determine the mechanical properties of these structures quantitatively. One of the primary challenges is the type of mechanical test and the scale at which relevant tests would have to be performed to yield meaningful information.

Mechanical testing is an essential part correlating cell wall chemistry and shape to growth and movement in plant cells and tissues. As a result, many mechanical testing techniques have been developed or adapted to study the mechanics of plant cell walls over the past two decades. Micro- and nanoindentation techniques (Bolduc *et al.*, 2006; Milani *et al.*, 2013; Peaucelle *et al.*, 2015; Routier-Kierzkowska *et al.*, 2012; Zerzour *et al.*, 2009), tensile testing (Phyo *et al.*, 2017; Saxe *et al.*, 2016; Zamil *et al.*, 2013), and various forms of acoustics-based microscopy (Gadalla *et al.*, 2014) have been used to this end. These techniques offer a spectrum of force and spatial resolution and each is associated with its own strengths and limitations. For instance, if the deforming force has out-of-plane components with regard to the plane of the specimen, as with indentation experiments, correlating the measured stiffness with in-plane properties of the cell wall is not always straightforward (Eder *et al.*, 2013; Milani *et al.*, 2013). Tensile testing allows for an in-plane stretch of the specimen and therefore, produces data that are more tangibly relevant for turgor induced stretch of the cell wall during cell growth. This aspect makes tensile testing a major mechanical test for the characterization of thin anisotropic primary plant cell walls.

Tensile testing of primary plant cell wall mechanics can be classified into two categories. In the first approach, the sample is stretched while either the force (creep test) or the length (relaxation test) is kept constant and the variations in the other parameter are monitored. This approach of tensile testing seeks to identify the time-dependent properties of the specimen. Creep test is the more prevalent type of testing in this category which is also referred to as extensimetry in some references. The creep approach is often employed to investigate the role of enzymes, temperature and other agents in the modulation of cell wall properties. Important conclusions have been drawn based on this on agents such as expansins and the influence of pH (Cosgrove, 1998; Durachko and Cosgrove, 2009). The second approach in tensile testing is to stretch the specimen until failure with the aim to extract passive mechanical properties such as stiffness, yield point or strength. The data from this approach are also relevant for cell growth since they can provide information on the orientation of cellulose and bonding of other wall polymers. For instance, tensile testing of adaxial onion epidermis has shown a higher stiffness parallel to the main axis of cell growth while in the transverse direction the tissue appeared to be more extensible. This tissue behavior is interpreted in terms of the mean

longitudinal orientation of cellulose microfibrils in cells of this tissue (Vanstreels *et al.*, 2005). Therefore, this approach of tensile testing can be used to study the cell wall anisotropy which, along with time-dependent enzymatic modification of the cell wall provides a full scenario under which the cell grows. The first approach and experiments related to cell wall extensibility are covered in Chapter 14.

In this chapter, we focus on the second approach, the classic tensile test. Tensile testing of plant specimens can be exploited to acquire essential information across multiple scales, from the organ-level to the subcellular scale. The plant root, for instance, requires cell wall pliability at the cellular level to grow, yet its overall material and structure should be able to withstand environmental stresses and be rigid enough to penetrate the soil without buckling. Therefore, the mechanical evaluation of root tissue can provide insight into its developmental stages and identify the parameters that a root should possess for the survival of the plant in a specific soil and environment. Chimungu *et al.* (2015) observed that the tensile strength of root specimens decreases with the diameter. It was shown that the tensile properties of the stele predominate the overall root tensile strength while the cortical properties such as cell count and thickness were shown to affect the bending and buckling properties of the root. Saxe *et al.* (2016) studied the effect of age on mechanics of the elongated zone in etiolated *Arabidopsis* hypocotyls. They correlated the mechanics of the elongated zone to material density, geometry and cellulose content. Their results suggest that the tensile stiffness of the samples may increase over a period of growth with no apparent increase in cellulose content implying a role for other components such as pectin (for related reading refer to Bidhendi and Geitmann, 2016; Phyto *et al.*, 2017). Such an interesting approach combining tensile testing with biochemical analysis enables unraveling the contribution of different wall biopolymers and cell shape to macroscale organ properties.

Tensile testing parameters and methods

Tensile testing requires gripping a specimen either at two ends (uniaxial testing) or its circumference or along two axes (biaxial testing) and applying a pulling force. Tensile testing can be performed under strain (or displacement) control or force (stress or load) control. In the former, the rate of opening of the device “jaw” or elongation of the specimen is regulated while in the latter the magnitude of the extending force is adjusted. These modes are not to be mistaken with creep or relaxation experiments where either the strain or stress is kept constant. Load application stretches the specimen, and upon release of the force it either returns to its original dimensions immediately (elastic deformation), remains at the stretch-induced dimension (plastic deformation), or slowly returns partially or fully to its original dimensions (viscoelastic or anelastic). During stretching, the force corresponding to the elongation is recorded. For a uniaxial tension test, the force-displacement data points are used to derive a stress-strain graph as:

$$\sigma = \frac{F}{A_0} \quad \text{and} \quad \varepsilon = \frac{L-L_0}{L_0}$$

σ and ε are engineering stress and strain. A_0 and L_0 are original cross-section area and length of the specimen prior to onset of the experiment. A typical stress-strain graph is depicted in Fig. 1A. The curve may consist of three main zones. A transient “toe” region may indicate initial straightening of the specimen or rearrangement of its load-bearing components. The elastic regime in which deformations are recoverable and stresses are proportional to strains is followed by the plastic zone where elastic and permanent deformations occur in parallel. It should be noted, however, that many

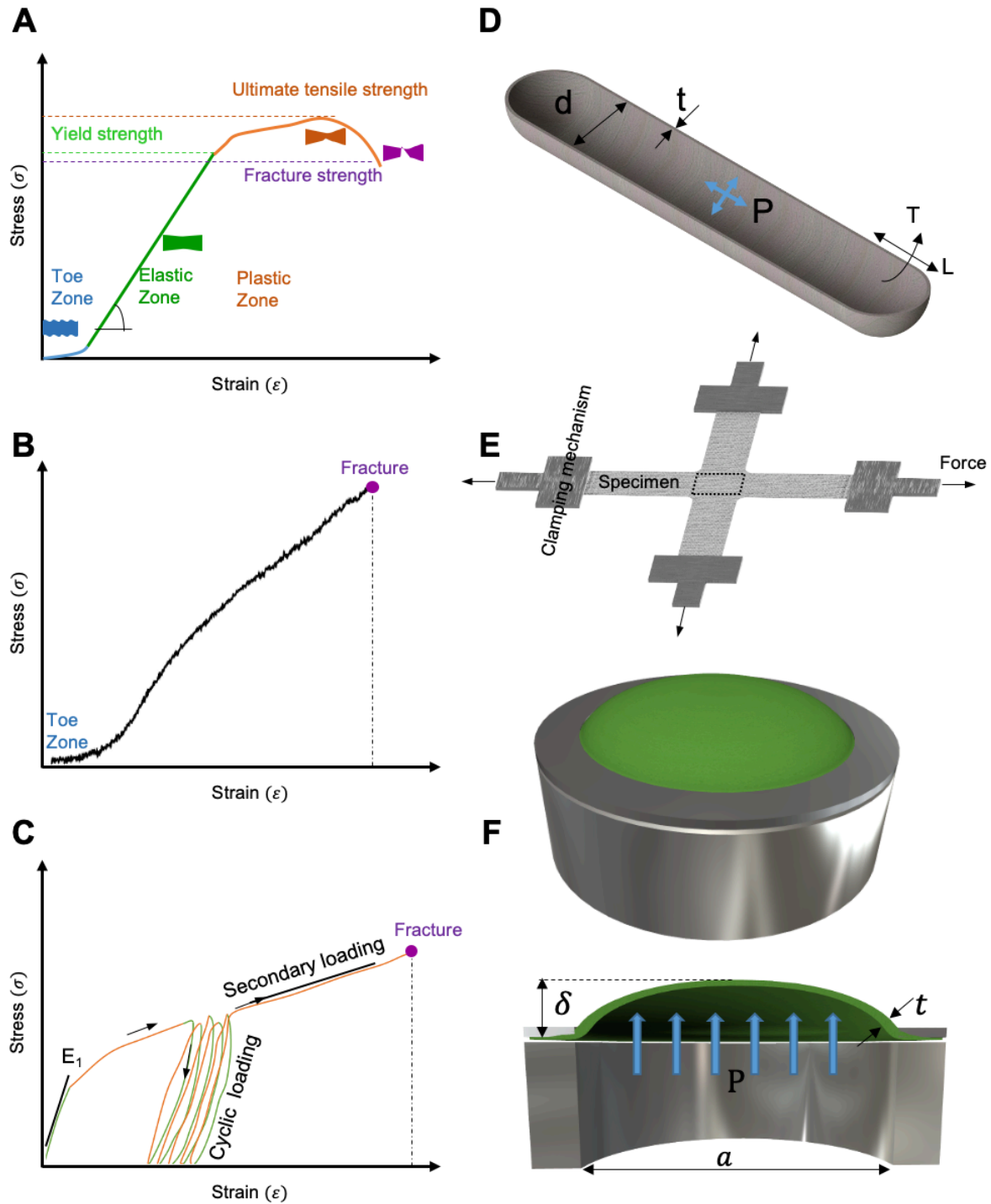


Figure 1: (A) Schematic of a typical strain-stress graph obtained from the tensile test. Various zones of material behavior are indicated. (B) Graph of experimental tensile test carried out on an onion tissue up to failure. (C) A generic cyclic tensile testing pattern applied to onion epidermal specimen similar to the study conducted by (Vanstreels *et al.*, 2005). The initial loading is followed by a number of loading-unloading cycles. The specimen is eventually loaded up to failure. (D) Cutaway view of a thin-walled cylindrical vessel under pressure (P), with a thickness of (t) and a diameter (d). T and L represent transverse and longitudinal directions, respectively. (E) Schematic of a biaxial tensile test cruciform specimen. (F) Bulge test of a flat specimen. The pressure gradient working on the specimen results in a hemispherical bulge of the sample. The displacement of the specimen at the center (δ), thickness (t), diameter (a) and the hydraulic pressure (P) are used to derive the material behavior of the specimen.

biological materials such as plant tissues, can exhibit considerably different stress-strain patterns with the marked zones either hard to distinguish or entirely absent (see the curve from a tensile test on onion epidermis in Fig. 1B). From this graph several mechanical parameters of the sample can be obtained. These parameters include the Young's modulus E , the yield strength σ_Y , the ultimate strength σ_U and the fracture strength σ_F . The Young's modulus indicates the material's resistance to deform and is determined from the slope of the linear reversible portion of the stress-strain curve. Yield strength corresponds to the stress values at which the specimen begins to deform permanently. This measure is often difficult to pinpoint precisely since plastic deformations can occur even at low strains. Ultimate tensile strength or simply tensile strength corresponds to the highest stress in the stress-strain graph. Fracture strength corresponds to the stress at fracture point. For materials exhibiting brittle fracture, tensile and fracture strengths can be close to each other. However, for ductile failure, the fracture strength is lower than the ultimate strength on a tensile testing graph based on "engineering" stress and strains. Other than engineering stress-strain curves, true stress-strain calculation accounts for changes in cross-section area of the specimen (generally a reduction) to calculate the stresses. This becomes more prominent in the plastic zone, at least for ductile materials with a tendency for necking (a phenomenon characterized by narrowing and a decrease in the cross-section of the specimen prior to failure; this is not to be confused with reversible lateral contraction of the material referred to as the Poisson's effect that occurs even in the small deformations in the elastic regime) (Fig. 1A). True stresses and strains can be calculated as:

$$\sigma_T = \sigma (1 + \varepsilon) \text{ and } \varepsilon_T = \ln (1 + \varepsilon)$$

In small strains, despite the lateral contraction of the specimen, the difference between the engineering and true graphs is negligible. However, beyond yielding and especially necking, the difference can be more dramatic. While the engineering stress in the specimen decreases after necking due to decrease in force required to stretch the sample, the true stress continues to increase since the effective cross-section is getting smaller in sample experiencing necking. Tensile tests allow for evaluation of the fracture behavior of the material and determination of fracture toughness. Fracture toughness is a measure of the resistance of the material against the propagation of existing cracks and tears. Such experiments can be carried out, for instance, by tension of a tissue with a preexisting notch. The area below the engineering stress-strain curve up to the elastic limit indicates the strain energy per volume stored and relates to "resilience", while if the curve is considered up to fracture, the area relates to tensile "toughness". Poisson's ratio, ν , measured at the elastic zone, provides information on the extent of the material shrinkage in directions perpendicular to that of the applied stress. Poisson's ratio can be determined based on:

$$\nu = - \frac{\varepsilon_{lateral}}{\varepsilon_{axial}}$$

$\varepsilon_{lateral}$ and ε_{axial} correspond to strains in perpendicular to and along the stress direction, respectively. Note that since most common materials contract laterally when stretched, $\varepsilon_{lateral}$ is negative and therefore the Poisson's ratio holds a positive value. Most isotropic elastic materials hold a Poisson's ratio between 0 and 0.5. In case of a near 0 Poisson's ratio, the material does not considerably strain laterally when strained axially. This applies for example to cork and is exploited in its application to seal bottles (Silva *et al.*, 2005). When squeezed, cork does not expand in other directions which facilitates its insertion into and removal from the bottle's neck. A Poisson's ratio of 0.5 refers to an incompressible material behavior, where the volume changes through longitudinal

increase and lateral contraction cancel each other out. For anisotropic materials, the Poisson's ratio differs based on the direction and, unlike for isotropic materials, the value is not confined to a particular range (Norris, 2006; Ting, 2004; Ting and Chen, 2005). It might be interesting to note that Poisson's ratio can even hold negative values. "Auxetic" materials with a negative Poisson's ratio, counterintuitively, expand in the transverse dimensions while being stretched uniaxially. This is often due to a particular internal structure, for example, that of the polymer network or shape of unit cells (Mir *et al.*, 2014). Auxetic materials are, however, rare in nature and are mostly synthetic. Most common materials including plant materials contract to compensate for elongation in the other dimension to preserve the volume. The magnitude of this contraction is correlated with the microstructure but also with the state of hydration. The presence of water in the porous network renders the material less compressible if the short force-exertion time or impermissible solid network prevent any water movement through the sample microstructure.

When plastic and elastic behavior occur combined, the components need to be distinguished to correctly deduce the mechanical properties. Experimentally, this can be achieved by closing the "jaw" of the tensile tester until the force read from the sensor reaches zero. The difference between the length at which the force becomes zero upon unloading and the mechanical zero at which the experiment started constitutes the permanent deformation. If further recovery eventually occurs, but not instantly, the material exhibits viscoelastic behavior. Most biological materials do exhibit viscoelastic behavior if given enough time. Therefore, whether to account for viscous effects is a matter of the time frame of the experiment and whether such a time frame is of biological relevance (i.e. may occur *in vivo*).

Uniaxial testing is experimentally easiest to achieve, and the obtained data are informative, certainly for plant organs that primarily grow longitudinally such as stems or roots. However, it is important to realize that even in uniaxially growing cells, the stress applied to the cell wall by the turgor pressure, and by the contact with other cells, is biaxial. Furthermore, a considerable mechanical anisotropy exists in the cell wall of elongating cells that promotes growth in preferential direction in the first place. Therefore, the mechanical characterization of plant materials and specifically plant cell wall by uniaxial testing may result in an incomplete representation of their overall mechanical behavior. Further, it has been shown for biological material such as arterial wall tissue—a collagen fiber-reinforced composite—that in uniaxial tests fibers can reorient toward the stress direction. This results in altered stiffness measurements in that direction when compared with biaxial tension test (Zemánek *et al.*, 2009). Indeed, recent studies on onion epidermis have demonstrated that during the uniaxial stretch of the sample, cellulosic bundles passively reorient toward the main direction of the stretch (Kafle *et al.*, 2017; Zhang *et al.*, 2017). A similar result was shown for cellulose microfibrils in wood cells (Keckes *et al.*, 2003). Another complicating factor in uniaxial tensile testing occurs when the stress is applied in a direction that does not align with one of the principal anisotropy axes. This can be the case when the anisotropy is not structurally evident, i.e. not correlated to the cell geometry. Off-axis loading of the anisotropic material results in the development of shear forces between the matrix components (e.g., between fibers and the matrix) in addition to tension. While this effect is also useful for the determination of shear strength of composite materials, it has been shown in a flax fiber composite that failure mechanism of the sample may vary dramatically based on the angle between the loading and the direction of anisotropy (Shah *et al.*, 2012). Therefore, the elastic modulus and failure parameters derived without knowledge of the tissue anisotropy require further attention.

Biaxial tension tests, in general, comprise two pairs of coaxially applied forces. Biaxial tension tests allow several important experiments such as the application of equal or different tension in two perpendicular directions or a stretch in one direction while the other direction is constrained. An *in vivo* way of applying biaxial tension to the walls of intact cells is to record the changes in cell dimension with and without turgor pressure. The changes in diameter and length of the cell can bear the elastic modulus (or moduli for anisotropic wall properties assumption) of the cell wall. For a thin shell pressure vessel ($\frac{t}{d} \ll 1$) (Fig. 1D) the resulting stresses along the two principal axes are:

$$\sigma_L = \frac{Pd}{4t} \text{ and } \sigma_T = \frac{Pd}{2t}$$

Where P is the internal (e.g., hydrostatic) pressure, t and d are the wall thickness and the diameter of the vessel, and σ_L and σ_T are longitudinal and transverse (hoop) stresses, respectively. It can be seen that the transverse stress is two times greater than the longitudinal stress simply due to the shape of the cell (for the same reason barbeque sausages split along their axis). From the inverse of the Hooke's law in three dimensions for an isotropic material and with plane stress assumption (variation in stress in thickness of the wall is negligible), it can be shown that:

$$\varepsilon_L = \frac{1}{E} (\sigma_L - \nu\sigma_T) \text{ and } \varepsilon_T = \frac{1}{E} (\sigma_T - \nu\sigma_L)$$

Where ε_L and ε_T are longitudinal and transverse strains. The strains can be determined from changes in dimension from microscopic images. The Poisson's ratio, however, needs to be measured separately or adopted from the literature. Approaching an incompressible behavior ($\varepsilon_L + \varepsilon_T + \varepsilon_{th} = 0$ with the subscript *th* denoting the direction of the wall thickness) corresponds to a Poisson's ratio value close to $\nu = 0.5$. However, as mentioned before, elongated cells rarely have an isotropic wall. In most cases, there exists a preferential orientation of cellulose microfibrils in the circumferential direction, although this may later change to a longitudinal direction due to passive reorientation during cell growth (Anderson *et al.*, 2010; Green, 1960). In such a case, the strains cannot be explained with a single Young's modulus. A special case of anisotropy, the transverse isotropy that corresponds to unidirectional composites can be relevant to the composition of plant cell walls with a relatively well-organized direction of fibers. Simplifying the inverse of Hooke's law written in form of strains for transverse isotropy and plane stress assumptions, the longitudinal and transverse strains can be written as:

$$\varepsilon_L = \frac{1}{E_L} (\sigma_L - \nu_{TL}\sigma_T) \text{ and } \varepsilon_T = \frac{1}{E_T} (\sigma_T - \nu_{LT}\sigma_L)$$

Where ν_{LT} and ν_{TL} are the Poisson's ratios. The subscript *LT*, for instance, denotes the Poisson's ratio effect in the transverse direction due to the strain in the longitudinal direction. In case of incompressible transverse isotropy, it can be shown that:

$$\nu_{LT} = \frac{1}{2} \text{ and } \nu_{TL} = 1 - \frac{E_L}{2E_T}$$

Therefore, the strain relationships can be further simplified to (for a more in-depth reading refer to classic books on the theory of elasticity or, for instance, see Argatov and Mishuris, 2015; Bernal *et al.*, 2011):

$$E_L = \frac{\sigma_T}{2\varepsilon_L + \frac{4}{3}\varepsilon_T} \text{ and } E_T = \frac{3}{4} \frac{\sigma_T}{\varepsilon_T}$$

Therefore, having measured the axial and transverse strains, Young's moduli in two directions can be calculated based on the above relationships. While this method allows for measurement of the elastic moduli of the cell wall along the two axes, it requires a measurement or a justified assumption of the turgor pressure. In the absence of quantitative information on turgor, the ratio of anisotropy ($\frac{E_L}{E_T}$) can be evaluated using this approach.

A common way of performing biaxial tension test for planar materials is to prepare square or cruciform shapes of the sample to be stretched by a pair of perpendicularly positioned actuators (Hannon and Tiernan, 2008; Lally *et al.*, 2004) (Fig. 1E). The elastic and plastic deformations are then analyzed in the midsection of the specimen which should remain stationary by proper adjustment of displacement actuators. Bulge testing is yet another common technique for tensile characterization of both thin and thick films (Small *et al.*, 1994; Srikar and Spearing, 2003; Yu *et al.*, 2016). It has the advantage of not requiring preparation of complex sample shapes or dealing with complex stress distributions in specimens. In the bulge test, the sample can be of circular or square shapes. The specimen is fixed at the open end of a tube and pressure is applied on one side (Fig. 1F). Usually, a positive pressure is applied, for instance, by using a viscous silicone oil that does not permeate the specimen (Chanliaud *et al.*, 2002), resulting in the outward bulge of the specimen into a hemispherical profile. Depending on the shape of the membrane specimen, various analytical solutions have been developed to correlate the parameters such as pressure (P), the maximum deflection of the specimen (δ), its diameter (a) and thickness (t) (for instance, refer to Maier-Schneider *et al.*, 1995). Alternatively, inverse FE modeling can be employed to identify the unknown parameters. The maximum deflection at the center of the specimen and the sample thickness can be measured using either tactile techniques or, without contact, through optical methods such as 3D digital image correlation (DIC), and plotted against the pressure of the fluid in the chamber (Machado *et al.*, 2012; Neggers *et al.*, 2014; Nouira *et al.*, 2014; Orthner *et al.*, 2010). This technique also allows for the determination of the Poisson's ratio of the sample. If the pressure is kept constant, the increase in the bulge size versus time can be used as a creep test to acquire viscoelastic properties of the specimen. Adopting this strategy, Chanliaud *et al.* (2002) performed uni- and biaxial tension tests to study the mechanical behavior of the cell wall under turgor pressure using *Acetobacter xylinus* based cellulose as plant cell wall analog. Cellulose, cellulose/pectin and, cellulose/xyloglucan composites were tested under tension and compared with FE modeling used to interpret the pressure-displacement test data.

Tensile testing setup

The tensile setup generally consists of two distinct compartments: sensors and actuator units. In this section we describe the essentials of a simple uniaxial tensing device. For biaxial testing, a significant number of considerably different configurations have been developed over the years (for instance, refer to a review by Hannon and Tiernan, 2008). However, the concepts remain similar to a great extent. The displacement is generated by a displacement transducer. A wide range of actuators can be used to this end such as mechanical, piezoelectric or pneumatic mechanisms (Fig. 2). In motorized lead screw actuators, for instance, rotation of the lead screw by a stepper motor causes linear displacement, similar to the driving mechanism of many syringe pumps. Finely threaded screws in conjunction with precise stepper motors allow for the production of displacements of several centimeters in range and submicrometer in resolution well-suited to displacements required in many micromechanical tensile tests. Several methods exist for measurement of displacement or strain in the specimen. The simplest method is to rely on the displacement values given as inputs to the

displacement transducer. However, different sources such as the existence of backlash in the gear system can cause a lag and cause the actual displacement to deviate from the desired input. As a result, the displacement input cannot be used to derive the stress-strain relationships and instead, the device's "cross-head" or "jaw" motion which is equivalent to the actual displacement of the actuator and the gripping ends can be measured and used. Using gripping end displacement as a measure of sample strain is usually accomplished by readings from a position sensor such as a linear variable differential transformer (LVDT). LVDTs consist of a ferromagnetic core that can move freely without contact in a hollow cylinder equipped with an assembly of a primary and secondary coils. The primary coil fed with an AC or DC input voltage induces a voltage in the secondary coils. The movement of the core, connected from one side to the displacement actuator or a gripping end, in or out of the hollow cylinder changes the amplitude and phase of the voltage induced in secondary coils which constitutes the output signal from the LVDT enabling measurement of that displacement. However, this reading does not take into account the compliance of the loading frame. The loading part of the device including the force sensor, extensions and fixtures can deform along with the specimen during the loading and result in an underestimation of the elastic modulus of the specimen (Sanders *et al.*, 1997). The frame compliance can be corrected for using a rigid mock-sample of known elastic modulus (Turek, 1993). Most times, the device compliance is considered to be a constant, meaning that a linear relationship between the force and the deformation of the loading apparatus is presumed (Sanders *et al.*, 1997). However, this might not always be the case, and nonlinearity might exist resulting in deviation of the measurements based on the specimen being used (Kalidindi *et al.*, 1997). Another method for strain measurements in tensile testing is the use of strain gauges. Strain gauges often but not always refer to thin film patches with an electrical resistance that changes when the patch is deformed (for an example of such a design refer to Pang *et al.*, 2012). Generally, strain gauges refer to the use of such contact patches although sometimes the term is also used for non-contact strain

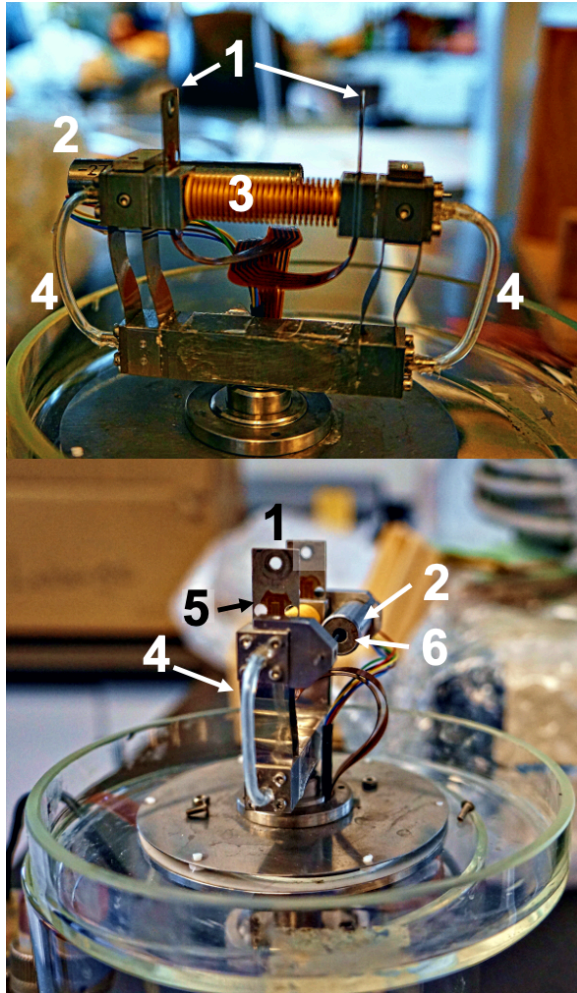


Figure 2: A miniaturized tensile testing device developed by Lynch and Lintilhac (1997) allowing for mechanical testing in air and liquid conditions. The testing chamber consists of (1) load shims, (2) LVDT (tube) (3) pneumatic bellows that act as displacement actuator opening or closing the frame driven by air flow (4) adjusted by a control unit based on displacement or force feedback. The deformation of the strain gauges (5) adhered to the load shims is read as the change in the output voltage and translated to forces acting to bend the shims. The displacement of the LVDT core (6) inside the tube reads the displacements.

measurement approaches (e.g., see Yamaguchi, 1981). There are numerous types of strain gauges based on their working mechanisms and the working environment they are intended for. However, the contact nature of the strain gauge requires it to be mounted and bonded to the surface of the specimen at various locations. The need for bonding to the specimen and the miniature size of most plant specimens render the use of strain gauges in plant tensile studies challenging. Further, the presence of strain gauges on the sample can affect the behavior of the specimen due to reinforcement or due to the weight of the patch and the connecting wires. Despite all these challenges, they only provide limited information on strains in the whole sample as the information is limited to the location of their installment. Therefore, strain fields and possible inhomogeneities and hotspots outside the installment zones remain undetected (Motra *et al.*, 2014; Soons *et al.*, 2012).

Extensometers can also make another class of strain measurement techniques. Basic contact extensometers rely on the attachment of a pair of “sensing arms” to two ends of the gauge length of the specimen averaging the strain over this region (for an example of its application refer to Boitier *et al.*, 2000). For plant applications, this method suffers from similar shortcomings as the strain gauges in that it affects the delicate sample and that only average strain data are produced. Non-contact extensometry approaches, on the other hand, seem very promising for specimens of various texture and sizes, especially in micro and nanomechanical characterization. Two broad classes of these methods rely on either image matching algorithms or optical interferometry. Matching algorithms such as DIC or differential digital image tracking (DDIT) techniques (Sharpe *et al.*, 2007) are based on analysis of consecutive images taken from the sample during the deformation. This is accomplished by means of one or more cameras (2D, 3D or volumetric) or by other techniques such as scanning electron microscopy (Kashfuddoja and Ramji, 2013). A sufficient number of speckles or patterns, either artificial or digital, for DIC (Lava *et al.*, 2009) or intensity peaks on the image for the DDIT are required for comparison and correlation of successive images to carry out full-field measurement of strains in the sample (e.g., Pan *et al.*, 2009; Sutton and Reu, 2017). DIC can provide a subpixel displacement/strain resolution (Hua *et al.*, 2007; Zhou and Goodson, 2001). Another advantage of an image-processing based approach is that rigid body motion (such as that occurring due to slippage of the specimen at clamps) can be accounted and corrected for. Various interferometry techniques have been developed for strain measurement. Electronic speckle pattern interferometry (ESPI), for instance, is one of the common interferometry methods for strain or displacement measurements. In this technique, the sample surface is illuminated with a coherent laser beam. The reflected laser forms a pattern on the image recording setup. Topographical information of the specimen can be acquired based on changes in the phase difference between the reflected and original laser beams that is caused by sample deformation or displacement (Soons *et al.*, 2012; Yang and Etemeyer, 2003).

Other than displacement actuator and sensors, force sensors comprise another compartment of the tensile device. Forces are measured by one or two load cells that are installed on the gripping ends. Load cells are commonly based on one or more strain gauges. The deflection of the load cell beam results in changes in the electrical resistance of the strain gauge incorporated into it and in turn to a change in the output voltage that is read through an amplifier. The compliance of the load cells can be measured for different loads during the calibration stage and prior to the experiment and be accounted for in the displacement measurements. It is good practice to calibrate the device for force and displacement after mounting all the extensions on which the sample will be fixed, or in case of any change in environmental temperature or humidity. Excluding the weight of the extensions and

loading frame from the force and displacement measurements is even more important in vertical setups.

Common challenges associated with tensile testing

While some mechanical tests such as nanoindentation are relatively easy to perform, correlating the force-displacement data from these tests to in-plane properties of the cell wall, and accounting for complex probe-sample interactions is not straightforward and sometimes demands cumbersome calculations. Tensile testing, on the other hand, is considered a test requiring relatively simple calculations for extraction of the parameters from the experimental data. However, carrying out the experiment itself can be accompanied by many challenges that begin with sample preparation and handling and extend to sample alignment and gripping. Some of these challenges are briefly discussed.

Measurement of the original values

Obtaining the mechanical parameters of the sample in a tensile test relies on the measurement of several independent variables such as displacement, force and dimensions of the specimen that serve as input for the calculations. The eventual outputs of the tensile test, i.e. stresses and strains, can be only as accurate as the measurements of the independent values allow. Above we commented on the practical aspects of the force and strain measurements. An important set of input variables used to calculate the tensile testing parameters includes the original length and cross-section area (through diameter or width and thickness) of the specimen. With minute plant specimens such as roots or shoots of *Arabidopsis*, measurements of the original dimensions are typically carried out using optical techniques such as microscopic visualization. The issue here is that, other than the considerable biological variability among samples, the errors in measurement of these dimensions can dramatically alter the conclusions of the study. This becomes significant in situations where small changes in the mechanics of the cells or tissues are being investigated through tensile testing. The changes in mechanical properties of the material over close time points might not be dramatic and could be masked by errors or uncertainties in the measurement of original dimensions. An example of how important the measurement of the initial dimensions can be, even if they add complexity, is provided in a study by Saxe *et al.* (2016) which tested *Arabidopsis* hypocotyls for their tensile properties. In this study, a subset of hypocotyl samples exhibited decreasing cross-sections with age while in other datasets, no significant age-dependency was observed. The environmental and growth parameters such as humidity and temperature, while able to affect the length of the growing hypocotyls, were shown to not significantly affect the cross-section. The authors calculated the stress based on dividing the force by the cross-section of hypocotyls, as it should be done. However, the biologically atypical reduction in diameter, whether caused by biological variation or other, may significantly influence the determined stress values thus making a clear-cut interpretation more difficult. While it goes without saying that an increased number of biological replicates will increase the reliability of the conclusions drawn from experimental data, it will also be helpful to define methods and protocols that ascertain precise, consistent and reproducible quantification of dimensions and other parameters with potential influence on the measured mechanical values.

Gripping

One of the prominent technical challenges associated with tensile testing, particularly for soft and small tissue specimens, is fixing the ends of the sample. Stress concentration and damage near the grip can result in premature failure of the specimen near the gripping ends. With cylindrical samples such as root, shoot or hook structures such as prickles and spines, the ends of the specimen can be tied using a resistant non-deforming thread such as Kevlar (for instance, refer to Gallenmüller *et al.*, 2015). However, this requires a certain minimum size of the sample and the thread compliance needs to be accounted for in calculations. Clamping or grips are one of the common methods to hold the ends of the tensile specimen. Various grades of sandpaper can be used between the specimen and the clamp to prevent slippage. Sometimes, a layer of a softer material is placed between the sample and clamping mechanism to reduce the risk of specimen damage (Hervy *et al.*, 2017). Clamp gripping methods tend to induce damage and are particularly prone to slippage, due to reasons such as the non-flat geometry of the samples and moisture. Further, in case of the model plant *Arabidopsis*, the minute size of its organs make solutions such as tying unviable. Piercing structures such as fishing hooks have also been used for tensile testing of soft tissue such as porcine arterial specimens (Lally *et al.*, 2004). More invasive gripping techniques such as fishing hooks inevitably result in failure of the tissue around the fixture and are better suited for determination of tensile modulus and not strength. Due to these reasons, application of fast-curing glues such as cyanoacrylate can represent an attractive alternative. A high viscosity glue is preferable to prevent diffusion into the specimen as it can dramatically alter the mechanical properties of the tissue. Still, using a glue is not without its challenges. The glued area tends to shrink upon curing which causes a prestress in the sample. This is easily observable as the force sensors begin to register increasing tensile forces as the glue is curing. Therefore, it is necessary to release this tension prior to the onset of tensile testing. This can be done by closing the “jaw” of the device up to a point that the force reads zero which can be set as the mechanical zero for displacement. Further, moisture on the hydrated tissue can hinder curing of the glue. Since the tissue needs to be kept constantly hydrated, if not thoroughly submerged in liquid, acquiring a perfect fusion in a reasonable time may not be trivial. As the dimensions get smaller in micromechanical tests, the importance of applying glue droplets small enough to prevent bleeding into the gauge length of the specimen becomes significant. In such scenarios, techniques such as platinum deposition have been used to fix the microscale specimen on the loading frame, for instance, to study a subcellular patch of the onion cell wall under the scanning electron microscope (Zamil *et al.*, 2013). Handling and mounting thin film specimens such as an epidermis is challenging since they are prone to wrinkles and folding that can affect the stress distribution in the sample. Water surface provides a substrate to hold the specimen without wrinkles until mounting. In a recent study on tensile testing of ultrathin films, it was shown that stiction forces such as van der Waals could constitute a gripping mechanism (Kim *et al.*, 2013), a promising approach for ultrathin plant layers.

Biphasic behavior, effects of the loading rate and preconditioning of the cell wall

An interesting note related to the tensile behavior of the plant cell wall is a reported “biphasic” or “bilinear” behavior in the stress-strain curve. Such behavior is described as the existence of two different slopes in the stress-strain curve that in some cases are associated with a primary and a secondary Young’s moduli (Pieczywek and Zdunek, 2014; Spatz *et al.*, 1999; Vanstreels *et al.*, 2005) (Fig. 1C). While the existence of a strain-dependent and nonlinear elasticity in the plant cell wall, as also observed in mammalian cells and tissues (e.g., refer to Fabry *et al.*, 2001; Guilak *et al.*, 2014;

Kollmannsberger and Fabry, 2011; Mofrad, 2009), is expected, the approach to demonstrate this “bilinear” behavior seems unclear. As seen in Fig. 1C depicting a generic form of such graphs, in these studies the second Young’s modulus suggesting a secondary elastic behavior is defined after a turning in the graph (likely due to yielding) and on the loading (as opposed to unloading) part of the stress-strain curve. Firstly, the slope of engineering stress-strain curves in tensile testing of many materials does change after yielding. The existence of a slope change in the graph *per se* does not indicate a secondary elastic modulus. Further, Young’s modulus is defined based on relatively small strains prior to yielding or upon separating the plastic deformations from the total strain (thus using the unloading data) and is strictly indicative of deformations that are elastic, ε_e (where total strain $\varepsilon_t = \varepsilon_e + \varepsilon_p$). However, in these studies, the loading path is marked for the secondary Young’s modulus during a monotonic loading and the deformation seems to be associated with considerable plastic strains. For regions that are not purely elastic, fitting of appropriate elastoplastic models or presenting the data in terms of moduli other than Young’s modulus such as tangent modulus, therefore, is more appropriate. Secondly, while in some studies the transition between the primary and secondary elastic behavior is demonstrated under relatively small strains (less than 5% strain in Spatz *et al.*, 1999), others have demonstrated these two values in a range of over 20% strains (Vanstreels *et al.*, 2005). Besides the monotonic tensile loading, cyclic loading is performed in some studies and seems to suggest that, when unloading paths are considered, the slope of the stress-strain curve remains relatively unaffected and comparable to initial cycles (Vanstreels *et al.*, 2005). Therefore, the existence of such bilinearity in the stress-strain behavior of the wall material needs further assessment through analysis of reversible deformations. Moreover, studies are required to look into underlying wall composition and structures that result in such a putatively biphasic behavior.

Viscoelastic materials exhibit a rate dependency in their deformation behavior. This means, the faster the deformation is applied, the stiffer the tissue appears to be. Such a strain-rate dependency can affect the measurement of stiffness, but also the strength and maximum strain at fracture. Higher loading rates can result in increased apparent stiffness, increased stress, but less strain at fracture (the specimen appears less extensible). It is therefore interesting to investigate to what extent the results obtained by stretching the plant cell wall at different loading rates are comparable. Further, in many cases involving tensile testing of soft tissues, the specimen is preconditioned prior to actual data collection. In many animal tissues, it can be observed that the loading and unloading paths do not coincide (hysteresis). The area between them corresponds to the dissipated energy due to viscous or plastic effects. Further, for some materials, the peak load for the same amount of strain appears to differ in each cycle. Therefore, to obtain reproducible results, the specimen is sometimes “preconditioned” prior to measurements, for calculation of the elastic modulus and tensile strength. This is not to be confused with preconditioning term used in other contexts such as cold acclimation of the plant or removal of turgor pressure before tensile testing. The preconditioning is carried out by repeating the loading and unloading cycles for a certain number of times to reduce the peak force variations and also to some degree the hysteresis prior to actual measurements (Lee *et al.*, 1984). For tendons and ligaments, it has been shown that preconditioning results in an increase in both stiffness and strength of the samples. This has been suggested to be due to an increase in recruitment or reorientation of collagen fibers resisting the tensile loads toward the force field (Miller *et al.*, 2012; Schatzmann *et al.*, 1998). To verify whether preconditioning has caused damage or a permanent deformation in the sample, the toe region of the force-displacement curve can be analyzed. An increase in the length of the toe region (i.e. the existence of some strain without a corresponding

force) may indicate permanent deformations in the specimen. The reorientation of fibers, that might also depend on their initial distribution to begin with, may render the preconditioning a questionable practice if original properties of the tissue are of interest. There is a considerable variation between the strains used to precondition the samples among various studies. While some advocate a fraction of the real testing strains for preconditioning strains, others suggest a full experimental strain to be used before actual data collection and, obviously, this treatment must be reported along with other experimental conditions (Cheng *et al.*, 2009). In case that preconditioning strains were observed to induce damage, either due to fatigue (failure in the material at stresses significantly lower than the ultimate and fracture strengths of the material due to repetitive loading) or simply exceeding the fracture strength, there is a need to settle for lower strains in the actual experiments.

Tensile testing of onion epidermis was also demonstrated to exhibit hysteresis in loading-unloading paths (Vanstreels *et al.*, 2005). The existence of such a load history dependency of the plant tissue is suggested to stem from the presence of wrinkles or adhesion of other structures on the onion sample that unfold and resolve over a number of cycles (Wei *et al.*, 2001). However, in addition to these potential artifacts, the hysteresis and rate dependency seem to be an inherent part of most biological tissues, including plant materials. Tensile testing of onion epidermis has also shown a considerable transient response in the first cycle; a significant difference in stress-strain values between the initial and later loading cycles (Kerstens *et al.*, 2001; Vanstreels *et al.*, 2005; Wei *et al.*, 2001). This phenomenon that might be due to plastic deformations of the matrix occurring in the first cycle, becomes even more interesting when considering the contrasting results reported for the onion epidermis. From the work of Wei *et al.* a more significant transient response is observable in onion epidermal strips stretched perpendicular to the cell axis compared to the longitudinal one. Other studies (e.g., Kerstens *et al.*, 2001) report the opposite. Since in these studies, this behavior is correlated with the composite material behavior of the cell wall, e.g., the orientation of cellulose microfibrils, further studies are required to address these different observations.

Effect of cellularity

A major factor that distinguishes the use of tensile testing for the mechanical characterization of plant specimens from common industrial materials is that plant tissues are made up of cells. Whether the aim is to determine tissue-level mechanical properties or to deduce the cell-level mechanical properties, the cellularity of the material incorporates a number of factors that need to be accounted for when interpreting the experimental data. An immediate consequence of the cellularity is the difference between the effective and geometrical cross-sections of samples. The effective cross-section is the one that bears the loads. For plant tissues, this area is not the same as the tissue cross-section. If cell wall-level properties are to be deduced from the results, measuring only the portion containing the cell walls by subtracting the void space of cell lumina and intercellular spaces from geometrical (tissue-level) cross-section can be beneficial. However, instead, this is often either avoided and the whole cross-section is used in the calculations. In cases where factors such as cell type, cell size and cell wall thickness are expected to be identical between samples, this is probably an acceptable simplification. In cases where any of these factors is different, a more granular approach should be considered. Saxe *et al.* (2016) estimated the cell wall density based on the hypocotyl's dry weight and its volume in the hydrated state.

Aside from the measurement of the effective cross-section outlined above, inferring the mean mechanical properties of individual cell walls from tissue-level tensile testing is not straightforward.

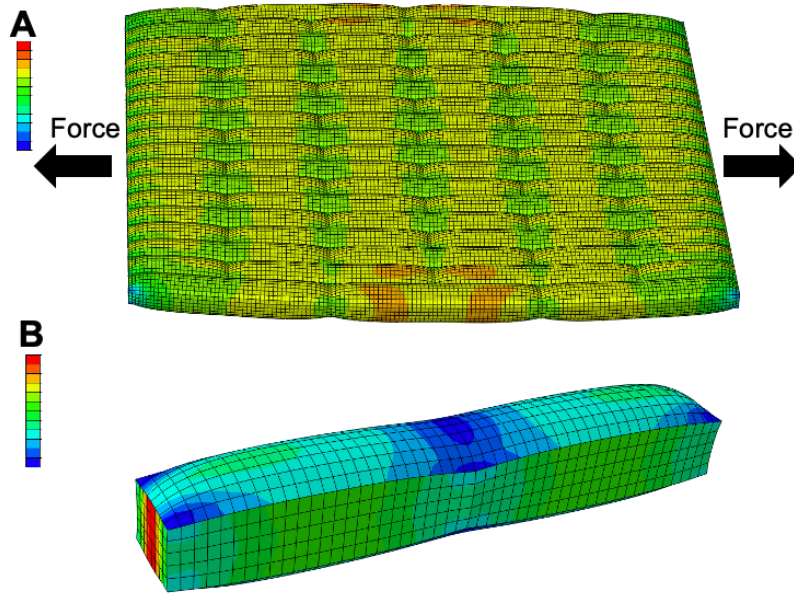


Figure 3: Finite element model of a tissue consisting of pressurized elongated cells. The distribution of stresses and strains is not uniform within the tissue (A), and can even vary in different walls of a single cell at subcellular scale (B). Color map represents the magnitude of principal stresses.

Firstly, due to the shape of the specimen, cellularity and presence of borders in the material, the stresses may not be distributed uniformly across the cells. This means that different cells in the tissue can experience different levels of stresses and strains. As a result, the properties of some cells may affect the calculations disproportionately, and the outcome of the tensile test may be a weighted rather than the arithmetic average of the properties of all cells. Additionally, even within a single cell, not all the walls experience the same share of stresses and can be stressed to a varying degree depending on their orientation with regard to the stress field and the cell geometry (Fig. 3). To what extent the mechanical properties of individual cells of different shapes and locations affect the overall elasticity of the tissue warrants further studies. Nevertheless, a study on onion epidermal cells has suggested that the growth anisotropy of the cells is correlated with tissue stiffness, with tissue samples with more elongated, higher aspect ratio cells appearing stiffer (Vanstreels *et al.*, 2005). While such differences are generally attributed to the anisotropic composition of the cell wall, it might be also due to cells shape. It should be noted that the apparent stiffness of a structure is determined in part by the properties of its building material, e.g. Young's modulus, porosity and degree of anisotropy, but also by the geometry of the structure. To better illustrate this, consider a beam with a rectangular cross-section under bending. It can be easily illustrated with a plastic ruler that the beam behaves stiffer under bending when placed with the longer edges of its cross-section vertical or parallel to the force (due to an increase of the second moment of area). Similarly, it is expected that the individual cells with different shapes resist the tissue-level deformation differently due to their geometry and orientation, affecting their contribution to overall mechanical properties of the tissue. This can confound comparison of the mechanical properties of different tissues with considerably different cell geometries if cell-level mechanical properties are to be inferred and correlated to tissue-level behavior. This issue concerns both classes of tensile testing outlined previously. Therefore, studies are required to untangle the contribution of cell geometry and material properties of the cell wall in the mechanical behavior that the tissue exhibits.

Tensile testing can be performed on both turgid and plasmolyzed cells. Turgid tissues are stiffer and reportedly fracture in a brittle manner. On one hand, tensile testing of turgid tissues is interesting since it more closely mimics the state of living plants. On the other hand, discriminating cell wall properties *per se* from the properties measured when under turgor induced tension requires a comparison between the two hydration states of the sample (Pieczywek and Zdunek, 2014).

Unraveling the mechanical properties of cell walls from the apparent tensile modulus obtained through tissue-scale mechanical characterization requires to also consider the intercellular interface, known as the middle lamella (Pieczywek and Zdunek, 2014; Zamil and Geitmann, 2017; Zamil *et al.*, 2017). In terms of tensile strength, the role of the middle lamella is intuitive. If tissue failure occurs by the failure at the middle lamella, i.e. cell separation or delamination, the strength of this structure determines the strength of the whole tissue. As explained by the weakest link concept, the fracture of the specimen is determined by the strength of its weakest spot (Freundthal, 1968). If and how the stiffness of the middle lamella also contributes to the tensile stiffness of the whole tissue remains elusive considering its negligible thickness.

To eliminate the compounding features such as cell shape and middle lamella, tensile testing on subcellular patches of the cell wall have been attempted (for instance, refer to Wei *et al.*, 2006; Zamil *et al.*, 2013). Besides the usual technical hurdles, manipulation and observation of the sample while keeping it hydrated are the major challenges at the micron scale. Given the challenges at each length scale, a combination of approaches incorporating macroscale response and micromechanics at the cell level is likely the most promising avenue in many cases. Multiscale experimental and computational strategies that combine tests both at the tissue and subcellular scale, giving consideration to the osmotic status, and integrating the experimental approach with numerical modeling allows for evaluation of the contribution of single cells to tissue-level mechanical properties and, conversely, determination of the cell-level properties from the tissue-level tension experiments. These considerations are equally important in the context of extensimetry and time-dependent studies where the goal is to quantify the effect of cell wall modifying treatments from the creep or relaxation of the whole tissue.

Nonuniform strain fields and application of optical strain measurement methods

Tensile testing of common industrial materials is often well documented and protocols regarding dimensions of the testing specimen, mounting and loading conditions are well defined. These dimensions and proportions are available in various standards provided by organizations such as ISO (International Organization of Standardization) or ASTM (American Society for Testing and Materials). Standards often ask for certain shapes of the specimen such as a so-called “dogbone” geometry or rectangular specimens of certain aspect ratios. The dogbone geometry incorporates a gauge length of a reduced cross-section in the middle part of the specimen and ensures that strains are mainly concentrated and uniform in that region rather than near the clamps. The specimen shape, boundary conditions and loadings prescribed in these standards ensure accurate and, importantly, reproducible results. In plants, however, the delicate nature of the samples, and the minute dimensions in many cases preclude production of such sample geometries. While some standards exist for tensile testing of thin papers and cardboards such as BS EN ISO 1924, relatively large dimensions, in the order of a few centimeters, are required that do not often correspond well with dimensions of plant tissues (Hervy *et al.*, 2017). Further, if strips need to be prepared, cutting the samples needs to be accurate without tears and flaws at edges that would cause stress concentration, premature failure and

influence the mechanical parameters obtained during the test. All samples to be compared should be of same dimensions or at least the gauge length undergoing tensile testing needs to be of same dimensions (Carew *et al.*, 2003; Tsuchiya *et al.*, 1998).

Due to lack of standardized protocols, a great variety of sample shapes (e.g., aspect ratios), often arbitrarily chosen, and even more variable testing conditions have been used for plant materials. Several studies have demonstrated the sensitivity of tensile testing results to sample dimensions, aspect ratio and geometry (Anssari-Benam *et al.*, 2012; Carew *et al.*, 2003; Hervy *et al.*, 2017). Further, due to errors introduced when measuring the strain based on the motion of the displacement transducer or the cross-head of the tensile device, different sample shapes can result in considerable differences in the calculated tensile modulus even within otherwise standardized samples. Hervy *et al.* demonstrated that measurement of stiffness of cellulose nanopapers shows a considerable dependence on sample geometry (Hervy *et al.*, 2017). The authors demonstrated that using the optical measurement of strain instead of the opening of the tensile device cross-head reduces the geometry-dependence in the estimated mechanical properties. This suggests that size-dependence in tensile testing is, at least in part, related to strain measurement (e.g., slippage). The tensile strength defined at failure theoretically does not depend on the specimen size. However, in practice, it has been observed that an increase in sample width can result in a decrease in tensile strength. This can be explained by the weakest link theory. As the width of the specimen increases so does the likelihood of inclusion of weak spots or defects in the sample (Hervy *et al.*, 2017). To add icing on the cake, the cellular nature of the plant tissues, as mentioned previously, and material anisotropy in individual cells, make the strain fields of plant specimens susceptible to inhomogeneity. As a result, the values reported by the force-displacement sensors may not be able to explain directly the phenomena occurring during a tensile test and comparing the mechanical properties of the biological specimens harvested at different stages of development or from tissues featuring intrinsically different cellular arrangement may be problematic. To fully address this concern, non-contact full strain field measurements can be used to acquire local information on the deformation of the sample. Optical extensimetry methods provide an attractive tool for the investigation of deformation within anisotropic and discontinuous materials such as intragranular and boundary movements in granular materials (Hall *et al.*, 2010). The displacement field in subregions of the specimen can be acquired by optical imaging and combined to construct the local strain information. The strain field data can be used to determine the mechanical parameters of the material using approaches such as virtual fields (Grédiac *et al.*, 2002; Promma *et al.*, 2009) or inverse FE method. Through comparing full-field displacement data with the predictions made by the FE model, material parameters can be reverse engineered. An FE model of the tensile test can be developed with inputs of the specimen dimensions (length, width, thickness) and force recorded from the sensors. The FE-produced displacement field is then compared with the displacement field of the landmarks or fiducial markers. The objective can be defined as the minimization of an error function based on the difference between the *in silico* and experimentally obtained values which results in the identification of the optimized parameters.

Optical extensimetry techniques are broad in their possible configurations as mentioned for DIC or interferometry approaches (Sutton and Reu, 2017). In the simplest form, they can be carried out by monitoring a few fiducial points on the specimen (such as two pairs of points in axial and transverse directions by Hervy *et al.*, 2017; or four symmetrically placed points in the middle of the square biaxial test specimen by Lally *et al.*, 2004). To increase the number of data points, fiducial markers such as fluorescent beads can be sprayed or fixed on the surface, ideally with a higher density

close to the middle and ends of the specimen. The tensile testing device can be placed under a stereo- or confocal microscope to record the displacement of fiducial markers versus the force exerted at two ends of the specimen. Kim *et al.* (2015) used fluorescent nanobeads as fiducial markers to calculate the microscale deformation of onion epidermis under tension. Application of optical methods in displacement/strain measurements is not limited to tensile testing. For instance, Armour *et al.* (2015) used fluorescent fiducial markers on the leaf epidermis of *Arabidopsis* to perform a time-lapse study of growth in epidermal pavement cells or Kuchen *et al.* (2012) used cell corners as landmarks to assess the local growth behavior of leaves.

Acknowledgements

Research in the Geitmann lab is funded by Discovery and Accelerator Grants from the National Science and Engineering Research Council of Canada and by the Canada Research Chair Program.

References

- Anderson CT, Carroll A, Akhmetova L, Somerville C. 2010. Real-time imaging of cellulose reorientation during cell wall expansion in *Arabidopsis* roots. *Plant Physiology* **152**, 787-796.
- Anssari-Benam A, Legerlotz K, Bader DL, Screen HR. 2012. On the specimen length dependency of tensile mechanical properties in soft tissues: Gripping effects and the characteristic decay length. *Journal of Biomechanics* **45**, 2481-2482.
- Argatov I, Mishuris G. 2015. Contact Mechanics of Articular Cartilage Layers: Asymptotic Models: Springer.
- Armour WJ, Barton DA, Law AM, Overall RL. 2015. Differential growth in periclinal and anticlinal walls during lobe formation in *Arabidopsis* cotyledon pavement cells. *The Plant Cell* **27**, 2484-2500.
- Baskin TI. 2005. Anisotropic expansion of the plant cell wall. *Annual Review of Cell and Developmental Biology* **21**, 203-222.
- Bernal M, Urban MW, Rosario D, Aquino W, Greenleaf JF. 2011. Measurement of biaxial mechanical properties of soft tubes and arteries using piezoelectric elements and sonometry. *Physics in Medicine and Biology* **56**, 3371.
- Bidhendi AJ, Geitmann A. 2016. Relating the mechanics of the primary plant cell wall to morphogenesis. *Journal of Experimental Botany* **67**, 449-461.
- Bidhendi AJ, Geitmann A. 2018. Finite element modeling of shape changes in plant cells. *Plant physiology* **176**, 41-56.
- Boitier G, Chermant J, Vicens J. 2000. Understanding the creep behavior of a 2.5 DC f-SiC composite: II. Experimental specifications and macroscopic mechanical creep responses. *Materials Science and Engineering: A* **289**, 265-275.
- Bolduc J-F, Lewis LJ, Aubin C-É, Geitmann A. 2006. Finite-element analysis of geometrical factors in micro-indentation of pollen tubes. *Biomechanics and Modeling in Mechanobiology* **5**, 227-236.
- Braybrook SA, Peaucelle A. 2013. Mechano-chemical aspects of organ formation in *Arabidopsis thaliana*: the relationship between auxin and pectin. *PloS One* **8**, e57813.
- Carew E, Patel J, Garg A, Houghtaling P, Blackstone E, Vesely I. 2003. Effect of specimen size and aspect ratio on the tensile properties of porcine aortic valve tissues. *Annals of Biomedical Engineering* **31**, 526-535.
- Chanliaud E, Burrows KM, Jeronimidis G, Gidley MJ. 2002. Mechanical properties of primary plant cell wall analogues. *Planta* **215**, 989-996.
- Chebli Y, Kaneda M, Zerzour R, Geitmann A. 2012. The cell wall of the *Arabidopsis* pollen tube—spatial distribution, recycling, and network formation of polysaccharides. *Plant Physiology* **160**, 1940-1955.

- Cheng S, Clarke EC, Bilston LE.** 2009. The effects of preconditioning strain on measured tissue properties. *Journal of Biomechanics* **42**, 1360-1362.
- Chimungu JG, Loades KW, Lynch JP.** 2015. Root anatomical phenes predict root penetration ability and biomechanical properties in maize (*Zea Mays*). *Journal of Experimental Botany* **66**, 3151-3162.
- Cooke JR, De Baerdemaeker JG, Rand RH, Mang HA.** 1976. A finite element shell analysis of guard cell deformations. *Transactions of the ASAE* **19**, 1107-1121.
- Cosgrove DJ.** 1998. Cell wall loosening by expansins. *Plant Physiology* **118**, 333-339.
- Cosgrove DJ.** 2005. Growth of the plant cell wall. *Nature Reviews Molecular Cell Biology* **6**, 850-861.
- Durachko DM, Cosgrove DJ.** 2009. Measuring plant cell wall extension (creep) induced by acidic pH and by alpha-expansin. *Journal of Visualized Experiments: JoVE*.
- Eder M, Arnould O, Dunlop JW, Hornatowska J, Salmén L.** 2013. Experimental micromechanical characterisation of wood cell walls. *Wood Science and Technology* **47**, 163-182.
- Fabry B, Maksym GN, Butler JP, Glogauer M, Navajas D, Fredberg JJ.** 2001. Scaling the microrheology of living cells. *Physical Review Letters* **87**, 148102.
- Forterre Y, Skotheim JM, Dumais J, Mahadevan L.** 2005. How the Venus flytrap snaps. *Nature* **433**, 421-425.
- Freundthal AM.** 1968. Statistical approach to brittle fracture. In: Liebowitz H, ed. *Fracture: an Advanced Treatise*, Vol. 2. New York: Academic Press, 591-619.
- Gadalla A, Dehoux T, Audoin B.** 2014. Transverse mechanical properties of cell walls of single living plant cells probed by laser-generated acoustic waves. *Planta* **239**, 1129-1137.
- Gallenmüller F, Feus A, Fiedler K, Speck T.** 2015. Rose prickles and Asparagus spines—different hook structures as attachment devices in climbing plants. *PLoS One* **10**, e0143850.
- Grédiac M, Toussaint E, Pierron F.** 2002. Special virtual fields for the direct determination of material parameters with the virtual fields method. 1—Principle and definition. *International Journal of Solids and Structures* **39**, 2691-2705.
- Green PB.** 1960. Multinet growth in the cell wall of *Nitella*. *The Journal of Cell Biology* **7**, 289-296.
- Guilak F, Butler DL, Goldstein SA, Baaijens FP.** 2014. Biomechanics and mechanobiology in functional tissue engineering. *Journal of Biomechanics* **47**, 1933-1940.
- Hall SA, Muir Wood D, Ibraim E, Viggiani G.** 2010. Localised deformation patterning in 2D granular materials revealed by digital image correlation. *Granular Matter* **12**, 1-14.
- Hannon A, Tiernan P.** 2008. A review of planar biaxial tensile test systems for sheet metal. *Journal of Materials Processing Technology* **198**, 1-13.
- Hervy M, Santmarti A, Lahtinen P, Tammelin T, Lee K-Y.** 2017. Sample geometry dependency on the measured tensile properties of cellulose nanopapers. *Materials & Design* **121**, 421-429.
- Hua T, Xie H, Pan B, Qing X, Dai F, Feng X.** 2007. A new micro-tensile system for measuring the mechanical properties of low-dimensional materials—Fibers and films. *Polymer Testing* **26**, 513-518.
- Kafle K, Park YB, Lee CM, Stapleton JJ, Kiemle SN, Cosgrove DJ, Kim SH.** 2017. Effects of mechanical stretching on average orientation of cellulose and pectin in onion epidermis cell wall: A polarized FT-IR study. *Cellulose*, 1-10.
- Kalidindi S, Abusafieh A, El-Danaf E.** 1997. Accurate characterization of machine compliance for simple compression testing. *Experimental Mechanics* **37**, 210-215.
- Kashfuddoja M, Ramji M.** 2013. Whole-field strain analysis and damage assessment of adhesively bonded patch repair of CFRP laminates using 3D-DIC and FEA. *Composites Part B: Engineering* **53**, 46-61.
- Keckes J, Burgert I, Frühmann K, Müller M, Kölln K, Hamilton M, Burghammer M, Roth SV, Stanzl-Tschegg S, Fratzl P.** 2003. Cell-wall recovery after irreversible deformation of wood. *Nature Materials* **2**, 810-813.

- Kerstens S, Decraemer WF, Verbelen J-P.** 2001. Cell walls at the plant surface behave mechanically like fiber-reinforced composite materials. *Plant Physiology* **127**, 381-385.
- Kim J-H, Nizami A, Hwangbo Y, Jang B, Lee H-J, Woo C-S, Hyun S, Kim T-S.** 2013. Tensile testing of ultra-thin films on water surface. *Nature Communications* **4**.
- Kim K, Yi H, Zamil MS, Haque MA, Puri VM.** 2015. Multiscale stress-strain characterization of onion outer epidermal tissue in wet and dry states. *American Journal of Botany* **102**, 12-20.
- Kollmannsberger P, Fabry B.** 2011. Linear and nonlinear rheology of living cells. *Annual Review of Materials Research* **41**, 75-97.
- Kuchen EE, Fox S, de Reuille PB, Kennaway R, Bensmihen S, Avondo J, Calder GM, Southam P, Robinson S, Bangham A. 2012. Generation of leaf shape through early patterns of growth and tissue polarity. *Science* **335**, 1092-1096.
- Lally C, Reid A, Prendergast P.** 2004. Elastic behavior of porcine coronary artery tissue under uniaxial and equibiaxial tension. *Annals of Biomedical Engineering* **32**, 1355-1364.
- Lava P, Cooreman S, Coppieters S, De Strycker M, Debruyne D.** 2009. Assessment of measuring errors in DIC using deformation fields generated by plastic FEA. *Optics and Lasers in Engineering* **47**, 747-753.
- Lee JM, Courtman DW, Boughner DR.** 1984. The glutaraldehyde-stabilized porcine aortic valve xenograft. I. Tensile viscoelastic properties of the fresh leaflet material. *Journal of Biomedical Materials Research Part A* **18**, 61-77.
- Lynch TM, Lintilhac PM.** 1997. Mechanical signals in plant development: a new method for single cell studies. *Developmental Biology* **181**, 246-256.
- Machado G, Favier D, Chagnon G.** 2012. Membrane curvatures and stress-strain full fields of axisymmetric bulge tests from 3D-DIC measurements. Theory and validation on virtual and experimental results. *Experimental Mechanics* **52**, 865-880.
- Maier-Schneider D, Maibach J, Obermeier E.** 1995. A new analytical solution for the load-deflection of square membranes. *Journal of Microelectromechanical Systems* **4**, 238-241.
- Milani P, Braybrook SA, Boudaoud A.** 2013. Shrinking the hammer: micromechanical approaches to morphogenesis. *Journal of Experimental Botany* **64**, 4651-4662.
- Miller KS, Edelstein L, Connizzo BK, Soslowsky LJ.** 2012. Effect of preconditioning and stress relaxation on local collagen fiber re-alignment: inhomogeneous properties of rat supraspinatus tendon. *Journal of Biomechanical Engineering* **134**, 031007.
- Mir M, Ali MN, Sami J, Ansari U.** 2014. Review of mechanics and applications of auxetic structures. *Advances in Materials Science and Engineering* **2014**.
- Mofrad MR.** 2009. Rheology of the cytoskeleton. *Annual Review of Fluid Mechanics* **41**, 433-453.
- Motra H, Hildebrand J, Dimmig-Osburg A.** 2014. Assessment of strain measurement techniques to characterise mechanical properties of structural steel. *Engineering Science and Technology, an International Journal* **17**, 260-269.
- Neggens J, Hoefnagels J, Hild F, Roux S, Geers M.** 2014. Direct stress-strain measurements from bulged membranes using topography image correlation. *Experimental Mechanics* **54**, 717-727.
- Norris A.** 2006. Extreme values of Poisson's ratio and other engineering moduli in anisotropic materials. *Journal of Mechanics of Materials and Structures* **1**, 793-812.
- Nouira H, Salgado J, El-Hayek N, Ducourtieux S, Delvallée A, Anwer N.** 2014. Setup of a high-precision profilometer and comparison of tactile and optical measurements of standards. *Measurement Science and Technology* **25**, 044016.
- Orthner M, Rieth L, Solzbacher F.** 2010. High speed wafer scale bulge testing for the determination of thin film mechanical properties. *Review of Scientific Instruments* **81**, 055111.
- Palin R, Geitmann A.** 2012. The role of pectin in plant morphogenesis. *Biosystems* **109**, 397-402.
- Pan B, Qian K, Xie H, Asundi A.** 2009. Two-dimensional digital image correlation for in-plane displacement and strain measurement: a review. *Measurement Science and Technology* **20**, 062001.

- Pang C, Lee G-Y, Kim T-i, Kim SM, Kim HN, Ahn S-H, Suh K-Y.** 2012. A flexible and highly sensitive strain-gauge sensor using reversible interlocking of nanofibres. *Nature Materials* **11**, 795-801.
- Peaucelle A, Wightman R, Höfte H.** 2015. The control of growth symmetry breaking in the Arabidopsis hypocotyl. *Current Biology* **25**, 1746-1752.
- Phyo P, Wang T, Kiemle SN, O'Neill H, Pingali SV, Hong M, Cosgrove DJ.** 2017. Gradients in wall mechanics and polysaccharides along growing inflorescence stems. *Plant physiology* **175**, 1593–1607.
- Piecznyek PM, Zdunek A.** 2014. Finite element modelling of the mechanical behaviour of onion epidermis with incorporation of nonlinear properties of cell walls and real tissue geometry. *Journal of Food Engineering* **123**, 50-59.
- Prasanna V, Prabha T, Tharanathan R.** 2007. Fruit ripening phenomena—an overview. *Critical Reviews in Food Science and Nutrition* **47**, 1-19.
- Promma N, Raka B, Grediac M, Toussaint E, Le Cam J-B, Balandraud X, Hild F.** 2009. Application of the virtual fields method to mechanical characterization of elastomeric materials. *International Journal of Solids and Structures* **46**, 698-715.
- Routier-Kierzkowska A-L, Weber A, Kochova P, Felekis D, Nelson BJ, Kuhlemeier C, Smith RS.** 2012. Cellular force microscopy for in vivo measurements of plant tissue mechanics. *Plant Physiology* **158**, 1514-1522.
- Sanders PG, Eastman J, Weertman J.** 1997. Elastic and tensile behavior of nanocrystalline copper and palladium. *Acta Materialia* **45**, 4019-4025.
- Saxe F, Weichold S, Reinecke A, Lisec J, Döring A, Neumetzler L, Burgert I, Eder M. 2016. Age effects on hypocotyl mechanics. *PLoS One* **11**, e0167808.
- Schatzmann L, Brunner P, Stäubli H.** 1998. Effect of cyclic preconditioning on the tensile properties of human quadriceps tendons and patellar ligaments. *Knee Surgery, Sports Traumatology, Arthroscopy* **6**, S56-S61.
- Shah DU, Schubel PJ, Clifford MJ, Licence P.** 2012. The tensile behavior of off-axis loaded plant fiber composites: An insight on the nonlinear stress–strain response. *Polymer Composites* **33**, 1494-1504.
- Sharpe W, Pulskamp J, Gianola D, Eberl C, Polcawich R, Thompson R.** 2007. Strain measurements of silicon dioxide microspecimens by digital imaging processing. *Experimental Mechanics* **47**, 649-658.
- Silva S, Sabino M, Fernandes E, Correlo V, Boesel L, Reis R.** 2005. Cork: properties, capabilities and applications. *International Materials Reviews* **50**, 345-365.
- Small MK, Daniels BJ, Clemens BM, Nix WD.** 1994. The elastic biaxial modulus of Ag–Pd multilayered thin films measured using the bulge test. *Journal of Materials Research* **9**, 25-30.
- Soons J, Lava P, Debruyne D, Dirckx J.** 2012. Full-field optical deformation measurement in biomechanics: digital speckle pattern interferometry and 3D digital image correlation applied to bird beaks. *Journal of the Mechanical Behavior of Biomedical Materials* **14**, 186-191.
- Spatz H, Kohler L, Niklas K.** 1999. Mechanical behaviour of plant tissues: composite materials or structures? *Journal of Experimental Biology* **202**, 3269-3272.
- Srikar V, Spearing S.** 2003. A critical review of microscale mechanical testing methods used in the design of microelectromechanical systems. *Experimental Mechanics* **43**, 238-247.
- Sutton M, Reu PL, eds.** 2017. International Digital Imaging Correlation Society: Proceedings of the First Annual Conference 2016: Springer International Publishing.
- Ting T.** 2004. Very large Poisson's ratio with a bounded transverse strain in anisotropic elastic materials. *Journal of Elasticity* **77**, 163-176.
- Ting T, Chen T.** 2005. Poisson's ratio for anisotropic elastic materials can have no bounds. *The Quarterly Journal of Mechanics and Applied Mathematics* **58**, 73-82.

- Tsuchiya T, Tabata O, Sakata J, Taga Y.** 1998. Specimen size effect on tensile strength of surface-micromachined polycrystalline silicon thin films. *Journal of Microelectromechanical Systems* **7**, 106-113.
- Turek DE.** 1993. On the tensile testing of high modulus polymers and the compliance correction. *Polymer Engineering & Science* **33**, 328-333.
- Vanstreels E, Alamar M, Verlinden B, Enninghorst A, Loodts J, Tijsskens E, Ramon H, Nicolaï B.** 2005. Micromechanical behaviour of onion epidermal tissue. *Postharvest Biology and Technology* **37**, 163-173.
- Wei C, Lintilhac LS, Lintilhac PM.** 2006. Loss of stability, pH, and the anisotropic extensibility of Chara cell walls. *Planta* **223**, 1058-1067.
- Wei C, Lintilhac PM, Tanguay JJ.** 2001. An insight into cell elasticity and load-bearing ability. Measurement and theory. *Plant Physiology* **126**, 1129-1138.
- Yamaguchi I.** 1981. A laser-speckle strain gauge. *Journal of Physics E: Scientific Instruments* **14**, 1270.
- Yang L, Ettemeyer A.** 2003. Strain measurement by three-dimensional electronic speckle pattern interferometry: potentials, limitations, and applications. *Optical Engineering* **42**, 1257-1266.
- Yu Z, Xu H, Chen H, Pei Y, Fang D.** 2016. Characterization Method of Thick Films Using the Bulge Test Technique. *Experimental Mechanics* **56**.
- Zamil M, Geitmann A.** 2017. The middle lamella—more than a glue. *Physical Biology* **14**, 015004.
- Zamil MS, Yi H, Haque M, Puri VM.** 2013. Characterizing microscale biological samples under tensile loading: Stress–strain behavior of cell wall fragment of onion outer epidermis. *American Journal of Botany* **100**, 1105-1115.
- Zamil MS, Yi H, Puri VM.** 2017. A multiscale FEA framework for bridging cell-wall to tissue-scale mechanical properties: the contributions of middle lamella interface and cell shape. *Journal of Materials Science* **13**, 7947-7968.
- Zemánek M, Burša J, Děták M.** 2009. Biaxial tension tests with soft tissues of arterial wall. *Engineering Mechanics* **16**, 3-11.
- Zerzour R, Kroeger J, Geitmann A.** 2009. Polar growth in pollen tubes is associated with spatially confined dynamic changes in cell mechanical properties. *Developmental Biology* **334**, 437-446.
- Zhang T, Vavylonis D, Durachko DM, Cosgrove DJ.** 2017. Nanoscale movements of cellulose microfibrils in primary cell walls. *Nature Plants* **3**, 17056.
- Zhou P, Goodson KE.** 2001. Subpixel displacement and deformation gradient measurement using digital image/speckle correlation (DISC). *Optical Engineering* **40**, 1613-1620.